Materials Science Forum Vols. 519-521 (2006) pp 1077-1082
online at http://www.scientific.net

Fatigue Behaviour in Fine Grained Aluminium Alloys

L.J. Venning[1,a], I. Sinclair[1,b] and P.A.S. Reed[1,c]

[1]Materials Group, School of Engineering Sciences, University of Southampton, Highfield, Southampton, SO17 1BJ, UK

[a]L.J.Venning@soton.ac.uk, [b]is1@soton.ac.uk, [c]pasr1@soton.ac.uk

Keywords: Fatigue, closure, spray formed aluminium, dispersoids

Abstract. The effects of alloy production method on microstructure and hence fatigue crack growth rate and fracture mechanism have been examined for a variety of fine-grained/high dispersoid Al-Li-Mg-Zr and Al-Li-Cu-Mg-Zr alloys. Microstructures have been assessed by scanning and transmission electron microcopy, together with electron back scattered diffraction pattern assessment. In these fine-grained/high dispersoid materials, high crack growth rates are seen in comparison to the traditional DC cast alloys, excepting a material with high volume fraction of shearable precipitate. The effects of fracture surface roughness and closure levels in determining crack growth rates has been assessed.

Introduction

Spray casting of Al-alloys is of significant interest, as such materials present valuable alternatives in available alloying ranges over traditionally manufactured materials, with the further possibility of producing near-net shape, as-cast components. For larger gauge sections, the potential to manufacture high strength, non heat treatable alloys is of particular value, exploiting a combination of solid solution strengthening, high dispersoid levels and fine grain structure, as employed in the mechanically alloyed AA5091 system [1]. However the fatigue crack growth resistance of these materials may not benefit from intrinsic and extrinsic contributions to propagation resistance [2] due to (i) decreased slip reversibility due to the presence of the dispersoids and (ii) limited roughness induced crack closure (RICC) due to both the fine grain-size and high dispersoid content. The present work involves a study of several fine-grained/high dispersoid content materials, with a view to assessing fatigue crack growth behaviour and the associated micro-mechanisms of failure. Fatigue fracture resistance has been assessed in terms of both intrinsic and extrinsic factors, including a detailed assessment of the role of RICC.

Materials

The materials used are listed in Table 1. Spraycast alloy 1 (SC1) is a high Zr variant of 8090 type alloys with a relatively high associated β' (Al_3Zr) dispersoid content [3], transmission electron microscopy (TEM) identified a typical β' size of 15-45 nm [4]. SC1 was supplied as a rectangular extrusion that had been solution heat treated at 540˚C for 1.5 h, cold water quenched, stretched 2% and naturally aged. This alloy was originally developed by Alcan International under the designation UL30. Fatigue test samples were produced in the L-S orientation and then aged for 12 h at 150˚C. A relatively high Li content results in the presence of shearable δ' (Al_3Li) precipitates of ~ 10nm diameter after heat treatment (confirmed by TEM). Electron back scattered diffraction (EBSD) showed strong <111> and <100> fibre textures across the whole extrusion section. A fine, predominantly equiaxed grain structure with typical grain widths of 3-5μm was seen.

Spray cast alloy 2 (SC2) is a non-heat-treatable Al-Mg-Li-Zr alloy [5] with a relatively high dispersoid content (β', as in SC1) and, due to a low Li content, a limited potential for δ' formation. β' particle diameters were identified as ~10nm by TEM. The material was spray formed by Oxford University and supplied as an upset forged disc, with fatigue specimens extracted in an R-C orientation. A moderate grain size of ~5-20μm was seen (equivalent to the through-thickness grain dimensions in conventional DC cast plate and sheet products) with a <101> fibre texture being identified.

5091 is an Al-Mg-Li mechanically alloyed material [6] offering an ultra-fine-grained microstructure, with relatively equi-axed grains of less than 1μm size, stabilized by dispersions of 20-50 nm Al_2O_3 and Al_4C. A number of rogue 2-50μm grains were also seen however, up to ~ 25% of the material bulk [7]. A relatively weak crystallographic texture was observed in the material. The alloy was originally developed by Inco Alloys Int. as IN-905XL, and supplied in the form of 50mm thick forged plate, with fatigue samples being taken in an L-S type orientation.

Conventionally DC cast 8090 was also assessed in damage tolerant condition T8151, extracted from 40mm plate. This had also received a 2% stretch/24h heat treatment at 150˚C, and contained a high volume fraction of shearable δ' with a grain size of 20-30μm in the through-thickness direction. A strong, predominantly brass texture was observed and fatigue specimens were taken in the L-S orientation.

Table 1: Specimen dimensions, grain size and material compositions (* = nominal composition)

	Specimen width, W [mm]	Specimen breadth, B [mm]	Span S [mm]	Grain size [μm]	Li [wt%]	Mg [wt%]	Cu [wt%]	Zr [wt%]	Other [wt%]	Al [wt%]
8090	15	10	30	20-30	2.2	1.1	1.0	0.1		Bal.
5091	12	10	30	<1	1.3*	4.0*	-	-	0.8 O*; 1.1 C*	Bal.
SC1	15	10	20	3-5	2.87	0.78	0.97	0.39	-	Bal.
SC2	11	10	20	5-20	1.15	5.31	-	0.28	-	Bal.

Experimental Method

Side-grooved single edge notched bend bars were tested at room temperature in 3 point bend at an R-ratio of 0.1 and frequency = 15 Hz, as shown in Fig. 1. Side grooves were introduced to ensure plane strain conditions along the crack front and to improve closure measurements by removing unrepresentative plane stress effects, as demonstrated by Xu et al [8]. Experimental values of crack growth rate, *da/dN*, and stress intensity factor, ΔK, were obtained using a stepwise load shedding technique. A fatigue crack was initiated from a starter notch and the applied ΔK value reduced in 10% steps after *da/dN* data had been obtained over at a distance of at least 0.5mm or 5 times the estimated monotonic plastic zone size. Mechanical compliance assessment of cracked specimens was carried out using a clip gauge with knife edge attachments to monitor the response of the crack opening displacement to the applied load, and hence to indicate the level of closure present (i.e. as a deviation from linearity in the mechanical compliance).

Fatigue fracture surface features were analysed via secondary electron imaging on a JEOL 6500 field emission gun scanning electron microscope (FEG-SEM) and surface profilometry (to measure areas of 2mm x 2mm at a 12.27μm step size). Optical assessments were also carried out upon mechanically polished and etched fracture surface sections.

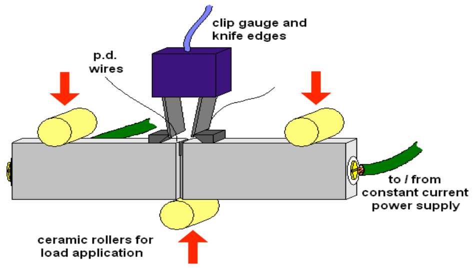

Figure 1: Experimental setup; 3 point bend loading of a sidegrooved specimen, with clip gauge for compliance assessment.

Results

Long crack fatigue testing. Results of the fatigue crack testing are shown in Fig.2, where the variation of *da/dN* against ΔK for the alloy systems of interest is compared. Fatigue crack growth behaviour of SC2 and 5091 are seen to be essentially equivalent, exhibiting relatively high growth rates *c.f.* SC1 and the alloy showing the best fatigue resistance, 8090 T8151. In the first instance it is evident that growth rates do not scale simply with grain dimensions, as SC2 has the coarsest grain size amongst the present fine-grained Al alloys. Closure can be assessed in terms of U, the ratio of the effective stress intensity factor ($\Delta K_{eff} = K_{max} - K_{op}$, where K_{max} and K_{op} are respectively the stress intensity factors at: (1) maximum load and (2) the load at which the crack is completely open, identified with onset of non-linear deviation in offset compliance curves) and the applied stress intensity factor, ($\Delta K_{app} = K_{max} - K_{min}$, where K_{min} is the stress intensity factor at minimum load). The variation of U with ΔK_{app} for all 4 alloys can be seen in Fig.3, where relatively low closure levels (U ~ 0.7-0.8) are seen in SC2 and 5091 *c.f.* significantly higher closure levels (U~ 0.1-0.2) in SC1 and 8090. Measured closure levels also vary with ΔK_{app} with the highest closure levels being seen at the lower ΔK_{app} levels.

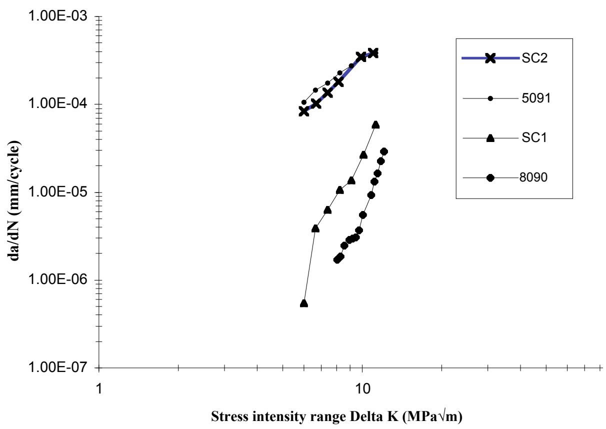

Fig. 2 *da/dN* vs ΔK comparison for all alloys

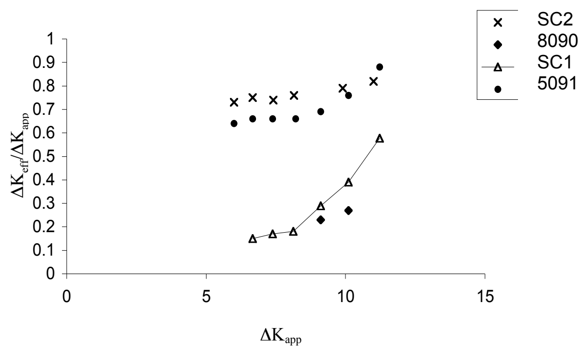

Fig. 3 U vs ΔK_{app} comparison for all alloys

Fractography. Macroscopic observations of the fine-grained materials (see Fig. 4), show the 5091 and SC2 have relatively uniform, fine-featured fracture surfaces, compared with the distinctly rough overall fracture surfaces of DC cast 8090 (e.g. see [6]). A more complex fracture surface morphology was however evident in the SC1 material, which was made up of 3 distinct regions: much of the fracture surface area was macroscopically flat and fine-featured, similar to the SC2 and 5091 surface observations, identified here as 'Region A'. 'Region B' was identified with visually rough surface regions: features were of ~1mm scale, with high local deflection angles, and an association with surface blackening characteristic of hydrated aluminium oxide formation via surface contact/rubbing [9]. Areas identified as 'Region C' showed low angle zig-zags from the nominal crack path, again at a length scale of ~1mm in the direction of crack growth. Region B features did not extend across the whole crack front, instead they formed distinct patches, surrounded by areas of Region A. Region C prevailed for ΔK levels below ~8MPa√m, at higher ΔK levels a mixture of Regions A and B was dominant. The overall shape and beach-marking of the fracture surfaces in these samples showed clear evidence of crack front pinning where Region B growth had occurred across the specimen cross-section.

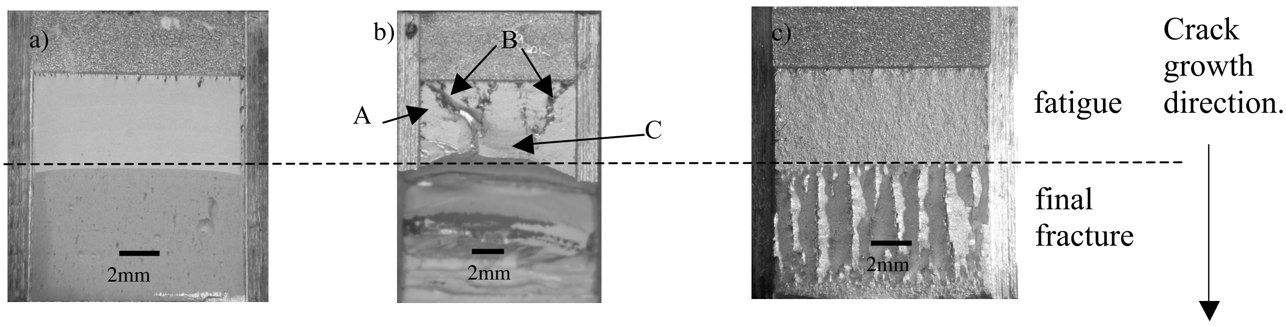

Figure 4: Overviews of fatigue fracture surfaces (a) 5091 (b) SC1 and (c) SC2

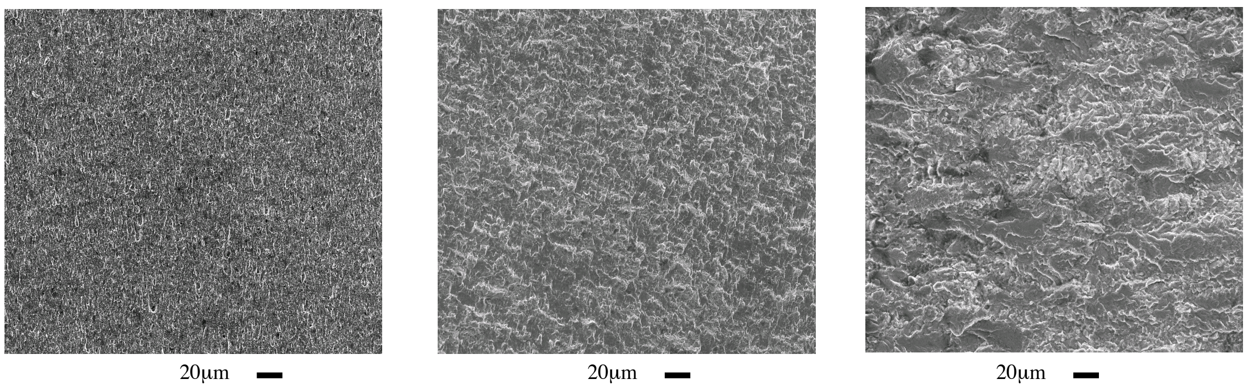

Figure 5: SEM examination of fatigue surfaces (a) 5091 (b) SC1 and (c) SC2

SEM observation shows typically very fine-scaled transgranular fatigue features on the 5091 and SC2 fracture surfaces as illustrated in Fig.5. The SC2 fracture surface features had the more coarse-scaled appearance of these three materials (in line with their larger grain size), but these regions are still distinctly fine-scaled *c.f.* the coarse, planar slip dominated faceting of the conventionally produced 8090 [6]. The final fracture surface of SC2 showed macroscopic vertical ridges and splits, corresponding to a 'crack-divider' effect, although this does not appear significant in the fatigue cracking process. The macroscopically flat 'Region A' of the SC1 fatigue fracture surfaces showed a fine transgranular appearance similar to the 5091 and SC2 materials. Pronounced faceting of the fracture surface was however evident in macroscopically rough areas of Region B. Talysurf profilometry confirmed the presence of distinctly rougher regions alongside the flat fine-scaled areas.

Discussion

Fatigue crack growth behaviour of SC2 and 5091 appear equivalent, with high crack growth rates *c.f.* SC1 and 8090. Whilst SC2 has a more moderate grain size *c.f.* the predominant sub-micron grain structure of the 5091, both alloys have little capacity for shearable precipitate formation, along with relatively high non-shearable dispersoid contents *c.f.* 8090. Grain size has little effect on crack propagation behaviour in these 2 systems in contrast to that reported in conventional Al alloys [10]. The combination of low shearable precipitate content and high dispersoid content could lead to relatively homogeneous slip, so reduced intrinsic crack growth resistance may be implied via reduced slip reversibility [2] whilst extrinsic contributions to crack growth resistance by RICC will be limited by an absence of slip band (i.e. faceted) crack growth. Recent modelling via both analytical and finite element methods [11,12] has produced estimates for fatigue closure based on local mixity conditions during crack propagation and corresponding residual shear strains in the crack wake. Details of the modelling are given in reference [11,12]; the closure predictions based on the analytical approach, using geometrical parameters from the Talysurf measurements of the fracture surfaces, are compared with actual closure measurements in Fig. 6. The overall predicted trend is decreasing closure with decreasing asperity size (at least for asperity sizes below the active plastic zone size). The closure predictions for SC1 are in the first instance based on Region B measurements, although it is recognised that this is only then representative of the regions of greatest RICC potential: high local closure levels in such regions is of course consistent with the local pinning seen in the crack front evolution.

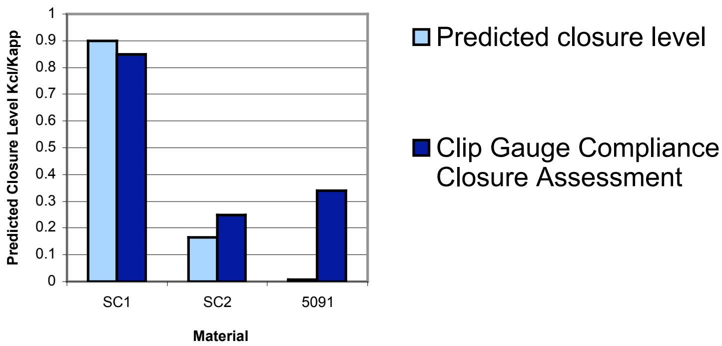

Figure 6: Comparison of closure predictions based on Talysurf measurements and actual closure measurements

Although SC1 has a finer grain size than SC2 and a higher dispersoid content (based on Zr levels) it clearly shows greater fatigue crack growth resistance and propensity for fracture surface roughness than either 5091 or SC2. The shearable precipitates in SC1 can then be identified with improved slip reversibility and reduced damage accumulation, whilst increasing slip band cracking and hence RICC contributions to crack growth resistance. These large crack deflections were not attributable to the presence of unusually coarse local grains (checked by sectioning and EBSD measurements), although the strong texture in SC1 might be considered to contribute to extended slip band formation over many grains. However the *fibre* texture that is present will not result in common plane orientations along which extended slip band crack growth might occur. EBSD assessment of the texture immediately behind the large deflections did not show any first order variation of local grain orientation, although a local increase in <111> to <100> component ratio was noted *c.f.* the overall texture.

Conclusions

High fatigue crack growth rates have been identified in two alloys with fine grain size and high dispersoid content, consistent with low closure levels due to the associated flat, transgranular fracture surface morphologies. The fine fatigue fracture surface features seen suggest a reduced influence of RICC on crack growth. In an alloy containing shearable precipitates (but still with fine grain size and high dispersoid content) behaviour appears controlled by an unusual mixture of microscopic and mesoscopic effects, with localized coarse crystallographic failure modes being observed. The large surface deflections are attributed to increased heterogeneous deformation due to the presence of shearable precipitates, overcoming the effects of high dispersoid and fine grain size. Overall it is found that RICC levels are reasonably predicted by recent analytical and FE modelling, and are consistent with the observed fatigue crack growth rate behaviour.

Acknowledgements

We would like to gratefully acknowledge financial support from the UK Engineering and Physical Sciences Research Council, MoD Defence Science and Technology Laboratory and QinetiQ. Oxford University supplied the spray-formed alloys studied as part of a collaborative research programme.

References

[1] H.R. Last, R.K. Garrett Jr, Metall. and Mater. Trans A Vol.27A (1996) pp737-745
[2] R.O. Ritchie, Mater Sci. Eng. A Vol. 103 (1988) pp15-28
[3] I. G. Palmer, J.W. Martin and B.Cantor, Proc. 3rd ASM Int. Conf. on *Synthesis, Processing and Modelling of Advanced Materials*, Paris (1997)
[4] A. Katsapi, personal correspondence, Imperial College (2005)
[5] S.C. Hogg, I.G. Palmer, P.S. Grant, Proc. ICAA9, IMEA (2004) p.325
[6] K.T. Venkateswara Rao and R.O. Ritchie, Int. Mater. Rev., Vol. 37 No.4 (1991) pp152-185
[7] S.C. Hogg, personal correspondence, Oxford University (2005)
[8] Y.G. Xu, P.J. Gregson and I. Sinclair, Mater Sci. Eng. A284 (1-2) (2000) pp114-125
[9] S. Suresh, Eng. Fract Mech.Vol.18 (1983) pp577-593
[10] R.D. Carter, E.W. Lee, E.A. Starke, and C.J. Beevers, Metall. Trans, A15 (1984) p555
[11] N. Kamp, M.R. Parry, K.D. Singh, I. Sinclair, Acta Mater, Vol. 52 (2) (2004) pp343-353
[12] M.R. Parry, S. Syngellakis and I.Sinclair, Mater Sci Eng A291 (2000) pp224-234